RMetS

ROYAL METEOROLOGICAL SOCIETY

Seasonal prediction of Korean regional climate from preceding large-scale climate indices

Maeng-Ki Kim,* Yeon-Hee Kim and Woo-Seop Lee
Department of Atmospheric Science, Kongju National University, Gongju, 314-701, Korea

Abstract:

On the basis of multivariate linear regression with an adaptive choice of climate indices as predictors, a seasonal forecast with a lead time of 2 months was applied to Korea on a monthly basis, and leave-one-out cross-validation was applied to obtain forecasting skill at the 1% significance level. The monthly ACC (anomaly correlation coefficient) skill was 0.42–0.65 for temperature and 0.35–0.63 for precipitation. COD (coefficient of determination) was 18–42% for temperature and 14–39% for precipitation. The first coupled SLP pattern related to Korean climate is very similar to the correlation pattern between the preceding climate index and SLP at the target month, indicating that preceding climate indices can be dynamically linked to Korean climate. For example, the PNA index at a lead time of 5 months prior to October is closely related to a circulation anomaly with weak negative correlation over the Okhotsk Sea to East Sea and strong positive correlation over a broad band from Lake Baikal to China. This SLP pattern provides conditions that can dynamically induce cold advection from northwestern Asia around Lake Baikal toward the Korean Peninsula, resulting in cooling over Korea. Copyright © 2006 Royal Meteorological Society

INTRODUCTION

Long-range forecasting is attracting increasing interest as society, industry and government attempt to minimize the risk, uncertainty and financial volatility associated with unseasonal weather (Lloyd-Hughes and Saunders, 2002). There are two basic approaches for long-range climate prediction: dynamic models and empirical statistical models. Although it is anticipated that dynamic models may become superior to empirical methods in future, empirical forecasts are still able to compete (Anderson *et al.*, 1999). Empirical statistical models have been developed based on the relationship between local/regional climate and preceding surface forcings such as SST, snow cover, and soil moisture (Colman and Davey, 1999; Lloyd-Hughes and Saunders, 2002; Blender *et al.*, 2003; Mo, 2003; Qian and Saunders, 2003; Kim *et al.*, 2004; Moura and Hastenrath, 2004; Singhrattna *et al.*, 2005), because the predictability of climate and weather at leads exceeding 10 days is linked to local and/or distant surface forcings and their feedback on the atmosphere (Palmer and Anderson, 1994; Goddard *et al.*, 2001). As shown in previous studies, the skill of empirical statistical models depends on the strong relationship between preceding large-scale predictors and regional-scale predictands. Climate indices useful as large-scale predictors have been developed to

express the variability of the atmosphere, land surface, and ocean at regional and global scales. These climate indices are widely used for seasonal predictions and are updated on a monthly basis by the climate diagnostics center (CDC) and climate prediction center (CPC). In this study, statistical seasonal prediction methods were developed and applied to the Korean climate using these regularly updated climate indices.

DATA AND METHODOLOGY

Data

The data used in this study are the monthly precipitation and temperature from 12 Korean weather stations for 50 years from 1954 to 2003 (Table I). The observed monthly mean SLP was obtained from the National Centers for Environmental Prediction (NCEP) and the National Center for Atmospheric Research (NCAR) reanalysis data with a horizontal resolution of $2.5° \times 2.5°$ latitude-longitude for 50 years from 1954 to 2003. The observed monthly climate indices were obtained from the CDC and the CPC for 51 years from 1953 to 2003. Monthly temperature anomalies for each month were computed by subtracting the long-term monthly mean from the detrended time series.

Many climate indices, which are updated monthly, are useful for seasonal prediction (Table II). For example, the arctic oscillation (AO), defined as the first leading

* Correspondence to: Maeng-Ki Kim, Department of Atmospheric Science, Kongju National University, Gongju, 314-701, ROK, Korea.
E-mail: mkkim@kongju.ac.kr

WILEY InterScience®
DISCOVER SOMETHING GREAT

Table I. List of Korean surface observation stations used in this study.

Station no.	Station	Latitude (°N)	Longitude (°E)
105	Kangnung	37.75	128.90
108	Seoul	37.57	126.97
112	Inchon	37.47	126.63
135	Chupungryoung	36.22	128.00
138	Pohang	36.03	129.38
143	Daegu	35.88	128.62
146	Jeonju	35.82	127.15
152	Ulsan	35.55	129.32
156	Kwangju	35.17	126.90
159	Pusan	35.10	129.03
165	Mokpo	34.82	126.38
168	Yeosu	34.73	127.75

mode from the EOF analysis of monthly mean height anomalies at 1000-hPa (Thompson and Wallace, 2000), is an important index for the prediction of regional climate in the middle latitude of the northern hemisphere. The Equatorial SOI (ESO), the Pacific Decadal Oscillation Index (PDO) and the Southern Oscillation Index (SOI) are also widely used for seasonal predictions in the Asian Pacific region (Rasmusson and Carpenter, 1982; Zhang *et al.*, 1997).

On the other hand, temperature (precipitation) just before the forecast time should be a good predictor for temperature (precipitation). In order to test this, we have calculated the auto-lag correlation for each target month (not shown). The result shows that there is almost no signal for precipitation while there are a few signals over

a lead month of 1 for temperature; for example, August with a lead month of 3, and September with a lead month of 4 and 5. However, we did not consider this variable for simplicity in this study.

Development of a multivariate linear regression model

The development of seasonal prediction models based on a multiple linear regression is very simple and popular for many regions. However, the process is not as simple as adding potential predictors to the regression model until an apparently good relationship is achieved, because an overfit regression can occur (Wilks, 1995). In this study, to avoid the possibility of overfitting the regression, we limited the number of predictors to five (about 25% of potential predictors). We also have considered multicollinearity in order to avoid the inflation of total variance explained by models. The firm separation of training and forecast periods is fundamental for true skill assessment. This distinction ensures that hindcasts are always applied to independent data, thus making the model skill the true forecast skill (Lloyd-Hughes and Saunders, 2002). In this study, we used more intensive criteria for verification, as explained in the sections on Cross-validation of the Model and Skill Scores of the Prediction Models.

Figure 1 shows the schematic diagram for the selection procedure for the seasonal prediction model. We developed forecasting models separately after separating the data into two groups. In Group I, the total period was divided into a training period of the initial 30 years and a verification period of the later 20 years, while the training period in Group II was the later 30 years and verification period the initial 20 years. As the first step, for each

Table II. List of potential predictors updated on a monthly basis from the Climate Diagnostic Center (CDC) and Climate Prediction Center (CPC), NOAA.

Abbreviation	Full name	Source
AMO	Atlantic Multidecadal Oscillation (Enfield *et al.*, 2001)	CDC[a]
AO	Arctic Oscillation (Thompson and Wallace, 2000)	CPC[b]
ESL	Equatorial Eastern Pacific SLP	CPC
ESO	Equatorial SOI	CPC
GML	Global Mean Land Ocean Temperature Index (Hansen *et al.*, 1999)	CDC
ISL	Indonesia SLP	CPC
MEI	Multivariate ENSO Index (Rasmusson and Carpenter, 1982)	CDC
NAO	North Atlantic Oscillation (Barnston and Livezey, 1987)	CPC
NOI	Northern Oscillation Index (Schwing *et al.*, 2002)	CDC
ONI	Oceanic Niño Index	CPC
PDO	Pacific Decadal Oscillation Index (Zhang *et al.*, 1997)	CDC
PNA	Pacific/North American Pattern (Barnston and Livezey, 1987)	CPC
SOI	Southern Oscillation Index (Rasmusson and Carpenter, 1982)	CPC
SWM	SW Monsoon Region Rainfall (Brasseur, 2001)	CDC
TNA	Tropical Northern Atlantic Index (Enfield *et al.*, 1999)	CDC
TSA	Tropical Southern Atlantic Index (Enfield *et al.*, 1999)	CDC
WHW	Western Hemisphere Warm Pool (Wang and Enfield, 2001)	CDC
WPO	West Pacific Oscillation (Barnston and Livezey, 1987)	CPC

[a] Climate diagnostics center.
[b] Climate prediction center.

Predictand
Y

Predictor
X_{ij}

Group (I, II)

Training Period

$$\hat{Y}_j = \sum_{i=1}^{n} \alpha_i + \beta_{ij-L} X_{ij-L}$$

< significant level 1% > NO

↓YES

Verification Period

$$\hat{Y}_j = \sum_{i=1}^{n} \alpha_i + \beta_{ij-L} X_{ij-L}$$
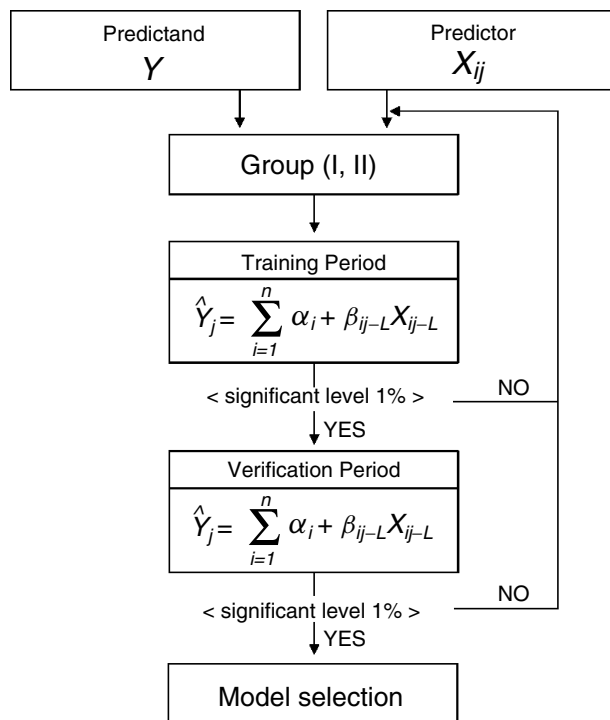
< significant level 1% > NO

↓YES

Model selection

Figure 1. Schematic diagram for the procedure of predictor selection to use in seasonal prediction. Subscripts i, j, and L represent predictor, target month, and lead month, respectively

calendar month and predictand X, the model fitting in Group I was performed separately using potential predictors of the preceding month from 2 to 12 months during the training period from 1954 to 1983 and then we performed significance tests for the verification period from 1984 to 2003. In each step, a 1% significance level was applied to go to the next step based on a two-tailed t-test for correlation coefficients between observed values and predicted (or fitted) values for each group. As the second step, we fit the Group I model during the training period from 1974 to 2003 using the same predictors from models obtained from the Group I significance test, and then performed significance tests for the verification period from 1954 to 1973. Thus, regression coefficients of each model in the second step are different from those

in the first step. It should be noted that the second step is just done in order to check the predictability of Group I models during the period of Group II. If the criterion was not satisfied, we changed the predictors or lead months until the criterion was satisfied. Thus, all combinations of predictors (two to five predictors) and lead months (2–12 months) were considered for each multiple linear regression. It should be noted that we did not use predictors at a 1-month lead because all of the potential predictors are updated in the middle of the month prior to the target month. Ultimately, we selected the first five models with the best correlation skill from Group I. This procedure was repeated to develop five models for Group II.

As an example, the results of October temperature and precipitation over Korea are presented and discussed in this study. Prediction skill in October is in the middle range among the 12 target months, as shown in Figures 2 and 3. Tables III and IV show predictors of ten models for October temperature and precipitation, respectively. The predictors of the Group I models are different from those of the Group II models, because we selected the best five models that have the highest correlation between prediction and observation in the verification period, not the training period, from each group. So, correlation skill during the verification period was higher than that during the training period as shown in Figures 2 and 3. In fact, in selecting prediction models on the basis of correlation skill in the verification period, predictors from each group were very similar except for one or two predictors. Although the five best Group I models did not rank among the five best Group II models, they met the requirements of the Group II verification test period. Moreover, the ensemble mean prediction from different predictors should be meaningful in detecting a signal for forecasting.

Figure 2(a) and (b) shows the ensemble mean temperature in October of the five models obtained from the two groups. Correlation coefficients between the ensemble mean and observations in Group I are 0.71 for the training period (1954 to 1983) and 0.85 for the verification period (1984 to 2003). In Group II, values were

Table III. List of preceding predictors used in ten seasonal prediction models for October temperature in Korea. Numbers in parenthesis represent leading months prior to October.

Group	Model no.	Predictors (lag)				
I	1	GML(11)	PNA(5)	SWM(8)	TNA(5)	WHW(10)
	2	AO(9)	ESO(3)	GML(11)	NOI(8)	WHW(6)
	3	AMO(6)	GML(11)	PNA(5)	SWM(8)	WHW(10)
	4	GML(11)	PNA(5)	SWM(8)	TNA(4)	WHW(10)
	5	AO(9)	ESO(3)	NOI(8)	TNA(9)	WHW(6)
II	1	AO(3)	NOI(8)	PDO(2)	PNA(10)	WHW(6)
	2	AMO(5)	GML(11)	MEI(8)	PNA(5)	SWM(8)
	3	ISL(11)	NOI(8)	PNA(10)	SOI(3)	WHW(10)
	4	AMO(5)	GML(11)	PNA(5)	SOI(9)	SWM(8)
	5	AO(12)	ISL(11)	NOI(2)	SWM(8)	WHW(10)

Table IV. List of preceding predictors used in ten seasonal prediction models for October precipitation in Korea. Numbers in parenthesis represent leading months prior to October.

Group	Model no.	Predictors(lag)				
I	1	AO(4)	NOI (2)	SOI (5)	SWM (6)	TNA (11)
	2	AO(4)	GML (3)	NOI (10)	PDO (8)	SWM (4)
	3	AO(4)	GML (2)	NOI (10)	PDO (8)	SWM (4)
	4	AO(4)	GML (6)	NOI (10)	PDO (8)	SWM (4)
	5	ISL(7)	NAO(5)	PDO(9)	TNA(9)	TSA(7)
II	1	GML(11)	ISL(7)	NAO(5)	PNA(9)	SWM(7)
	2	GML(11)	ISL(7)	NAO(5)	PDO(8)	SWM(7)
	3	ESL(7)	NOI(6)	PDO(6)	PNA(6)	TNA(9)
	4	ISL(7)	NAO(5)	PDO(8)	SWM(12)	TSA(7)
	5	ESL(12)	NOI(11)	PDO(8)	SWM(12)	WPO(2)
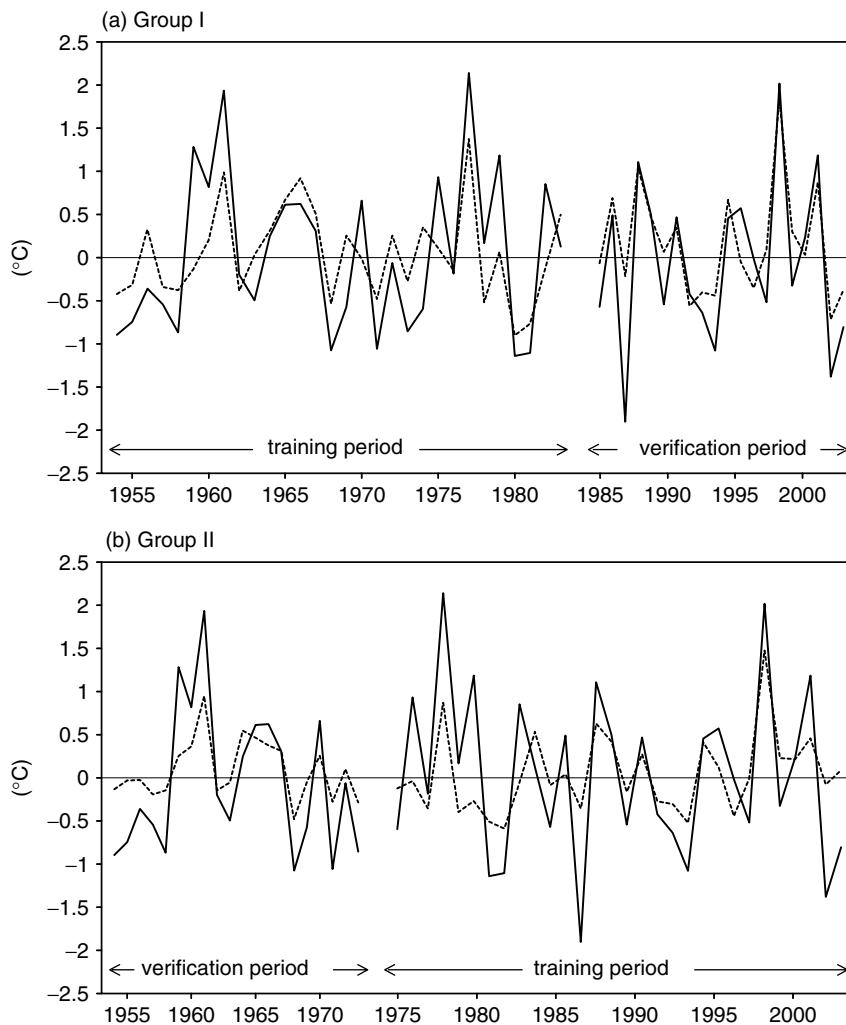
Figure 2. Time series of the observed (solid line) and ensemble mean of the five predicted (dashed line) October temperatures in Korea for Groups I (a) and II (b)

0.72 for the training period (1974 to 2003) and 0.90 for the verification period (1954 to 1973). Although several peaks in observation are underestimated in the statistical models, model prediction closely follows the inter-annual variations of the observations. The correlation skill for October precipitation was lower than that for October temperature: 0.66 for the Group I training period and 0.86 for Group II training period *versus* 0.85 for the Group I verification period and 0.70 for the Group II verification period, respectively (Figure 3).

Cross-validation of the model

We performed another verification procedure using ten statistical models selected from Groups I and II.
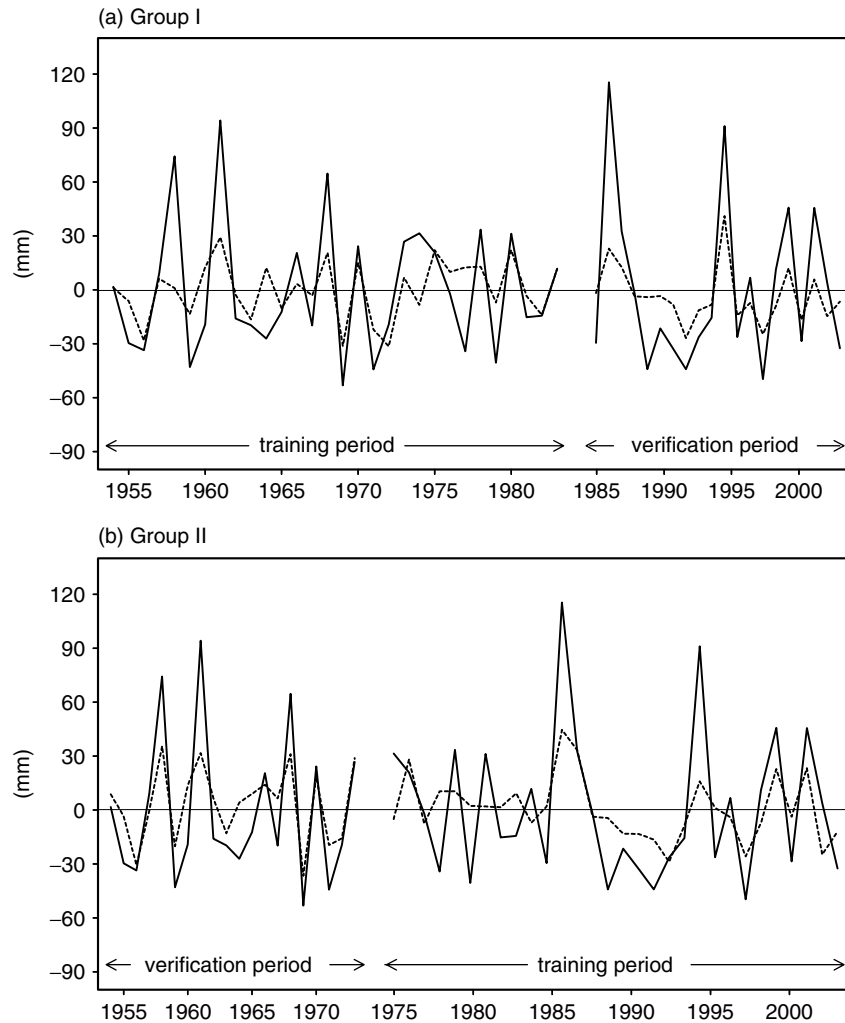
(a) Group I

(b) Group II

Figure 3. Time series of the observed (solid line) and ensemble mean of the five predicted (dashed line) October precipitations in Korea for Groups I (a) and II (b)

Cross-validation is very often carried out using developmental data sets of size n-1, and verification data sets contain the remaining single observation of the predictand (Wilks, 1995). In this case, there are clearly n distinct partitions of the data and n similar forecast equations. Thus, we can use all n observation samples of the predictand to estimate the prediction skill as explained in Figures 4 and 5. For small samples, the leave-one-out cross-validation (Michaelsen, 1987) is appropriate and has been applied in other statistical forecast models (Barnston, 1994). The relative performance of the forecast is measured by two skill scores, the anomaly correlation coefficient (ACC) and coefficient of determination (COD) (Wilks, 1995).

$$ACC = Cov(X,Y)/(S_X S_Y) \qquad (1)$$

$$COD = SSR/SST \qquad (2)$$

where $Cov(X,Y)$, S_X, and S_Y indicate covariance between predictor X and predictand Y, and the standard deviations of X and Y, respectively. SST and SSR represent the total sum of squares and regression sum of squares, respectively. Qualitatively, coefficient of determination

(COD) can be interpreted as the proportion of the predictand variation that is 'accounted for' by the regression model (Wilks, 1995).

RESULTS

Coupled modes between observed SLP and regional climate over Korea

In this section, we investigated how preceding predictors are related to atmospheric circulation around the Korean Peninsula in the target month of October. As an example, we chose a PNA (5) predictor for temperature and AO (4) for precipitation (Tables III and IV), because they are two of the most frequently appearing predictors in Group I.

Figure 4 shows the correlation pattern between PNA (5) and the observed October SLP. Weak negative correlations are seen over the Okhotsk Sea to East Sea, while strong positive correlations with significance levels between 1 and 5% are found only over the broad band from Lake Baikal to China. This indicates that positive
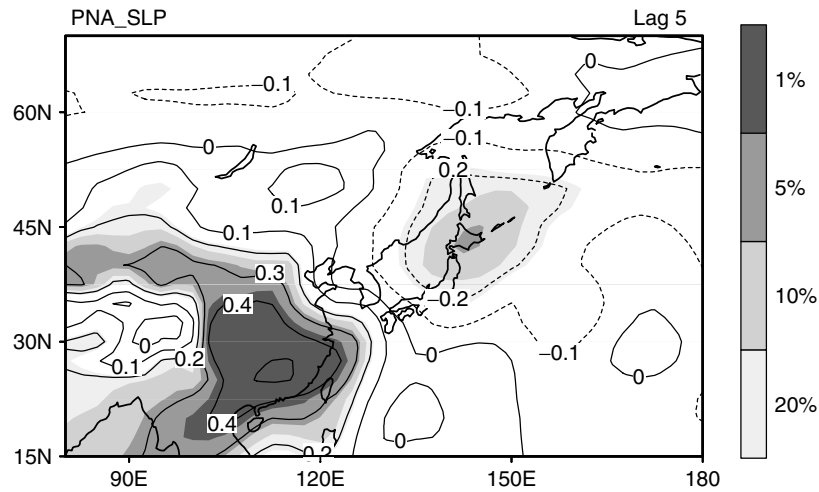
Figure 4. Correlation pattern between observed PNA index at lead month of five and observed SLP in October. The significance levels are shown with different shading on the right side
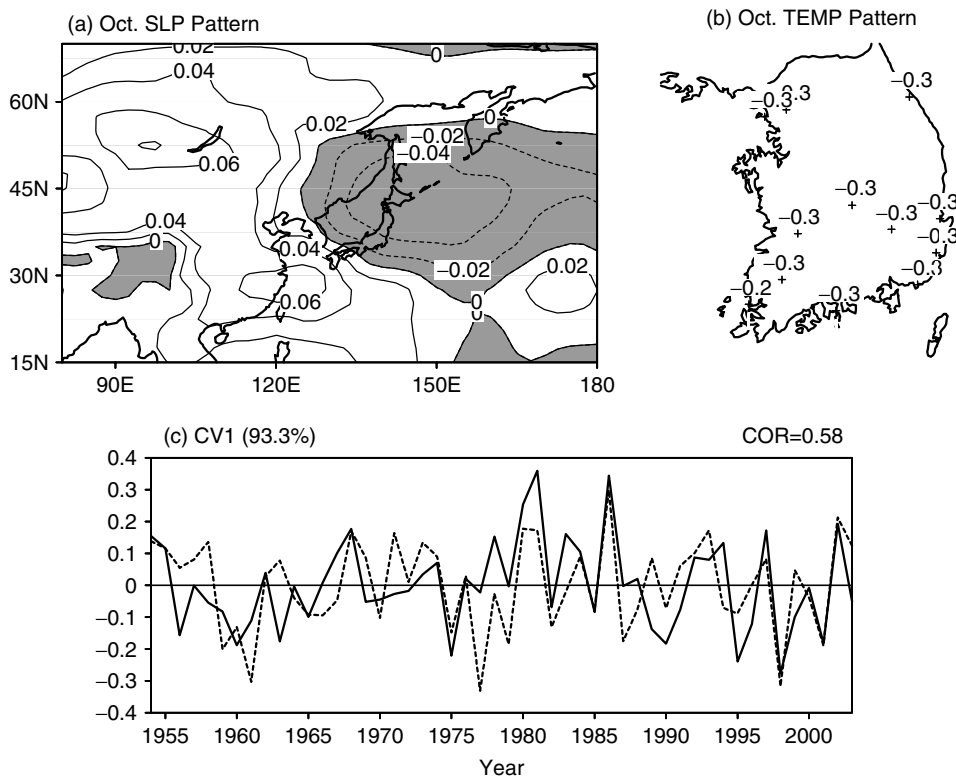

Figure 5. First leading SVD mode of observed SLP (a) and Korea temperature (b) in October. This mode explains 93.3% of total covariance. (c) Associated time coefficients of observed SLP (solid line) and Korea temperature (dashed line)

PNA (5) induces an east–west SLP anomaly in October around the Korean Peninsula, and the SLP pattern has conditions favorable to cooling the Korean Peninsula through cold advection.

Figure 5 shows the first singular value decomposition (SVD) mode between the observed SLP and October temperature over Korea. The correlation between the expansion coefficients is 0.58 (Figure 5(c)) and this mode accounts for 93.3% of total covariance. The main signals in the SLP pattern appear over the northwestern Pacific, Siberia, and the Yangtze River, corresponding to the

position of a typical air mass around the Korean Peninsula in October. There is an east–west SLP pattern around the Korean Peninsula and October temperature has the same negative sign over the entire region of Korea. This pattern represents a dynamic link that is physically reasonable, because Korean temperature decreases when anomalous anticyclonic circulation over East Asia intensifies, while cyclonic circulation over the western north Pacific intensifies. The SLP pattern of Figure 5(a) is very similar to the correlation pattern in Figure 4, especially in the northwestern Pacific with a negative correlation center around
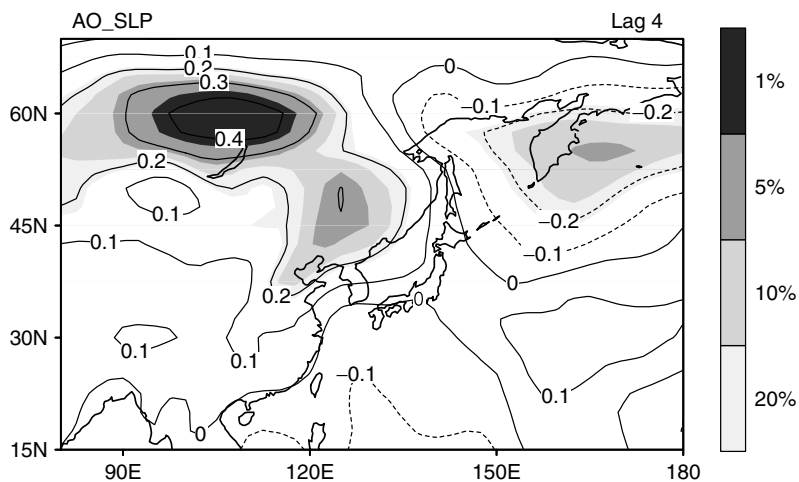
Figure 6. Correlation pattern between observed AO index at 4 lead months and observed SLP in October. The significance levels are shown as different shading on the right side
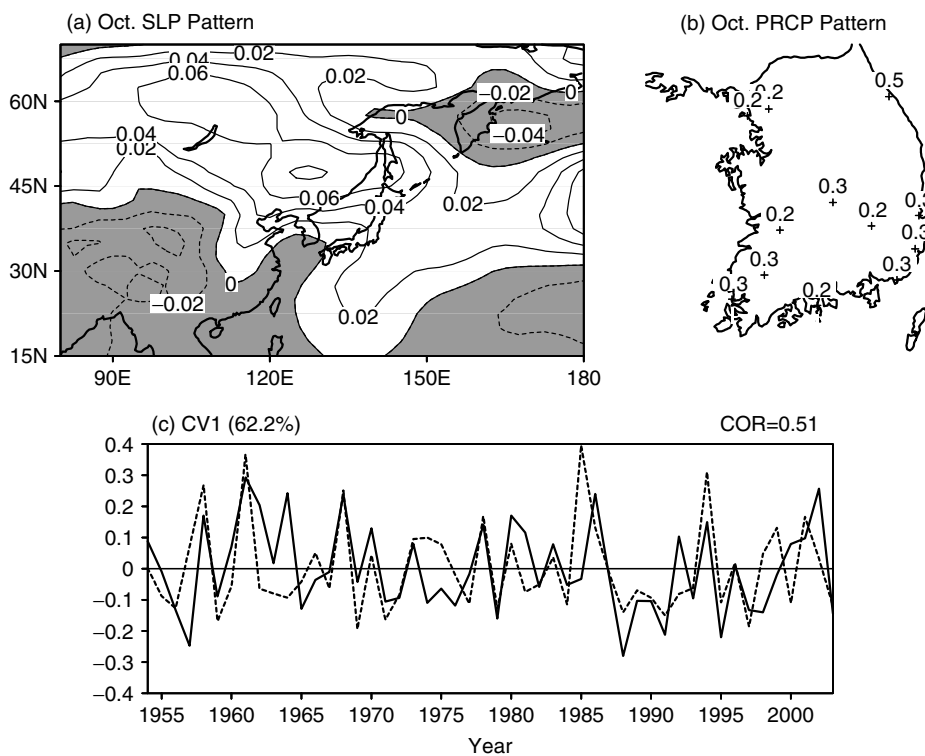

Figure 7. First leading SVD mode of observed SLP (a) and Korea precipitation (b) in October. This mode explains 62.2% of total covariance. (c) Associated time coefficients of observed SLP (solid line) and Korea precipitation (dashed line)

Okhotsk Sea and a strong positive correlation center in a broad band from Lake Baikal to China, indicating that PNA (5) may induce a circulation anomaly that ensures a dynamic link between the observed SLP and temperature.

Figure 6 shows the correlation pattern between AO (4) and the observed SLP in October. Strong positive correlation over a 5% significance level appears in the region from Siberia to China while strong negative correlation appears around the Kamchatka Peninsula. This correlation pattern is very similar to the first coupled mode between the observed SLP and Korean precipitation as shown in Figure 7(a). In fact, the western wing of

the Aleutian Low, one of the important pressure systems during the cold season, including October, is extended to the Kamchatka Peninsula, and its variability is also large over the Kamchatka Peninsula (not shown). The Siberian High also gradually takes its place over the region of Lake Baikal to China before winter. The strengthening of the Siberian High, especially over the northern Korean Peninsula, may induce cold advection and associated large latent heat flux over the East Sea between Korea and Japan. This pattern provides conditions that supply moisture to the Korean Peninsula. We can confirm this dynamic link from Figure 7(b) which shows all positive
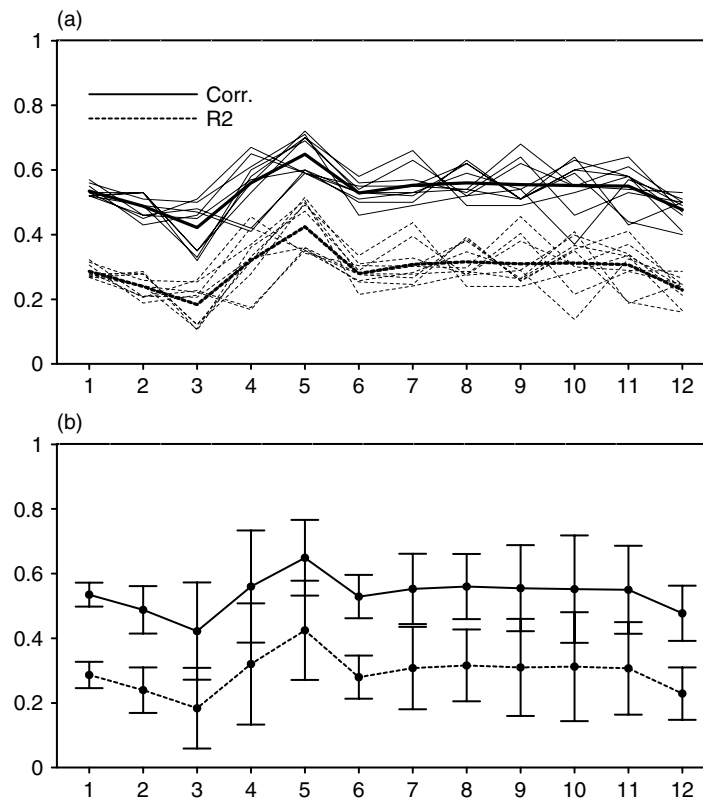
Figure 8. Forecast skill (a) and standard deviation (b) of ten models shown in Table III for Korean temperature. Solid and dashed lines represent ACC and COD, respectively. The heavy solid line represents the ensemble mean of the ten models. The total height of error bar includes approximately 95% when a Gaussian distribution is roughly provided

signals in the precipitation pattern over Korea. Temporal correlation between the two time series also shows a close connection, with a correlation coefficient of 0.51.

We have compared correlation pattern by each index with the leading SVD modes. The results show that correlation pattern by a common index among indices of ten models is very similar to that of the SVD pattern while in other indices it is partially matched with each other.

Skill score of the prediction models

In this section, the monthly forecasting skill, estimated by leave-one-out cross-validation in each segment, is investigated at a 2-month lead time using ACC and COD. It should be noted that prediction models used in this section have already passed through the first step of validation as explained above. Thus, the leave-one-out cross-validation may provide a strong criterion, especially in the short-total period of this study.

Figure 8 shows the forecast skill and standard deviation of ten models for Korean temperature (Table III). Monthly ACC (heavy solid line) ranged from 0.42 in March to 0.65 in May, and monthly COD was 18–42% of total variation of temperature (Table V). During the pre-monsoon season, May has one of the highest skills. The start of the rainy period, June, has low skill because of the uncertainty about the exact starting time of the rainy period; while during the rainy period, July has the

highest skill. On the other hand, the cold season (November to March) has lower skill, about 0.42 to 0.55 ACC, than the warm season (Table V), implying that statistical models do not fully explain the large variability of temperature during the cold season.

Figure 9 shows the forecast skill and standard deviation of ten models for Korean precipitation (Table IV).

Table V. The ensemble mean skill of ten prediction models for anomaly correlation coefficient (ACC) and Coefficient of determination (COD). The critical ACCs at the 5 and 1% significance level are 0.28 and 0.36, respectively, based on a two-tailed t-test.

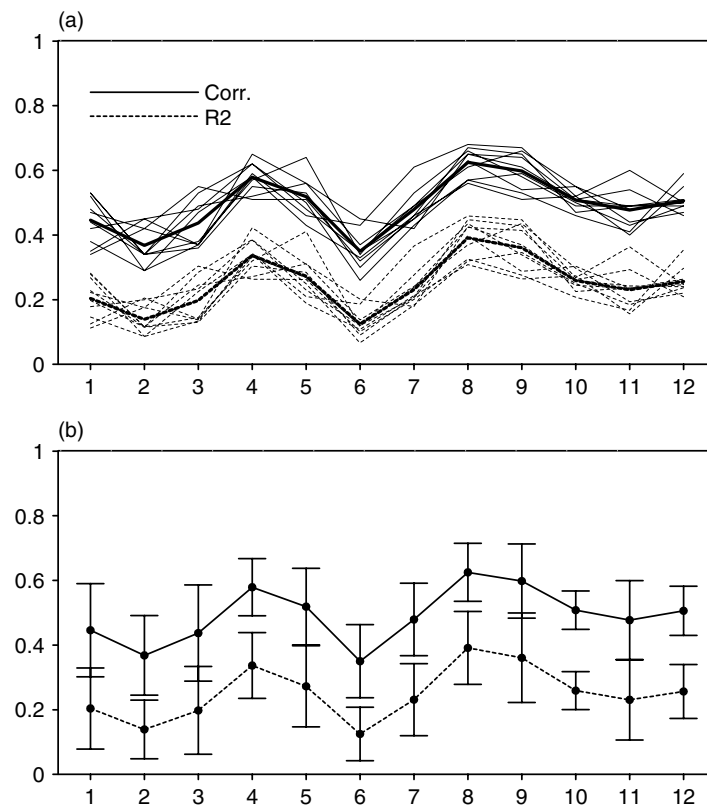| Month	Temperature		Precipitation	
	ACC	COD	ACC	COD
January	0.54	0.29	0.45	0.20
February	0.49	0.24	0.37	0.14
March	0.42	0.18	0.44	0.20
April	0.56	0.32	0.58	0.34
May	0.65	0.42	0.52	0.27
June	0.53	0.28	0.35	0.12
July	0.55	0.31	0.48	0.23
August	0.56	0.32	0.63	0.39
September	0.56	0.31	0.60	0.36
October	0.55	0.31	0.51	0.26
November	0.55	0.31	0.48	0.23
December	0.48	0.23	0.51	0.26

Figure 9. Forecast skill (a) and standard deviation (b) of ten models shown in Table III for Korean precipitation. Solid lines represent ACC and dashed lines represent COD. The heavy solid line represents the ensemble mean of ten models. The total height of error bar includes approximately 95% when a Gaussian distribution is roughly provided

Seasonal variation of ACC and COD resembles that of temperature in most months, as explained in Figure 8, although skill peaks in April and August. The overall correlation skill of precipitation is lower (within ±0.1) than that of temperature, especially during the rainy season (Table V).

CONCLUSION

In this study, we developed a seasonal forecasting model based on the multivariate linear regression with an adaptive choice of predictors using regularly updated climate indices. The available sets of the preceding predictors from 2 to 12 months are the monthly climate indices, which are updated monthly by the CDC and the CPC. The leave-one-out cross-validation was applied to obtain forecasting skill at a 1% significance level. The skill of forecast models and their significance levels are also discussed using ACC and the COD on a monthly basis.

The monthly ACC skill ranged between 0.42 and 0.65 for temperature and between 0.37 and 0.63 for precipitation. The COD ranged between 18 and 42% for temperature and between 14 and 39% for precipitation. The ACC skills are significant at the 1% significance level. The monthly ACC skill showed seasonal dependency, i.e. high skill during the warm season from April to September, except for June, and low skill during the cold season

from October to March. June has a low ACC of 0.53 and COD of 28% because of the variability in the starting time of the monsoon rainy season. However, after the end of the rainy season, the highest ACC skill of 0.63 and COD of 39% occurred in August for precipitation. March temperature has the lowest ACC skill of 0.42 and COD of 18%, and February precipitation has the lowest ACC skill of 0.37 and COD of 14%. These results are comparable with those of Kang and Baek (1993) and Kim (2003), obtained from the statistical model based on an empirical lagged relationship between the climate variables and the pre-season large-scale predictors, i.e. sea level pressure, sea surface temperature, and geopotential height. However, it is relatively easy to interpret physical meaning based on climate indices and extensible to long-lead time in this method.

The first coupled SLP pattern related to Korean climate is very similar to the correlation pattern between preceding climate index and SLP in the target month, indicating that preceding climate indices can be dynamically linked to Korean climate. For example, the PNA index at a 5-month lead time before October is closely related to a circulation anomaly with weak negative correlation over the Okhotsk Sea and strong positive correlation over a broad band from Lake Baikal to China. This SLP pattern provides conditions that can dynamically induce cold advection from northwestern Asia around Lake Baikal toward the Korean Peninsula, resulting in cooling over Korea.

Despite considerable recent progress, our understanding of climate forcings and how they feedback to influence climate variability and predictability at different leads and over different predictand timescales remains far from complete (Qian and Saunders, 2003). The physical mechanism of how large-scale climate indices in preceding months induce circulation anomaly at the target month remains an open question requiring further investigation by numerical modeling. Although it is possible that statistical models will continue to be competitive with or even superior to numerical models for the seasonal prediction problem, it is difficult to gain a complete physical understanding of the climate system through statistical models, indicating that the development of increasingly realistic numerical models may increase understanding of physical processes.

ACKNOWLEDGEMENT

REFERENCES

Anderson J, van den Dool H, Barnston AG, Chen W, Stern W, Ploshay J. 1999. Present-day capabilities of numerical and statistical models for atmospheric extratropical seasonal simulation and prediction. *Bulletin of the American Meteorological Society* **80**: 1349–1361.

Barnston AG. 1994. Linear statistical short-term climate predictive skill in the northern hemisphere. *Journal of Climate* **7**: 1513–1564.

Barnston AG, Livezey RE. 1987. Classification, seasonality and persistence of low-frequency atmospheric circulation patterns. *Monthly Weather Review* **115**: 1083–1126.

Blender R, Luksch U, Fraedrich K, Raible CC. 2003. Predictability study of the observed and simulated European climate using linear regression. *Quarterly Journal of the Royal Meteorological Society* **129**: 2299–2313.

Brasseur O. 2001. Development and application or a physical approach to estimating wind gusts. *Monthly Weather Review* **129**: 5–25.

Colman A, Davey M. 1999. Prediction of summer temperature, rainfall and pressure in Europe from preceding winter North Atlantic Ocean temperatures. *International Journal of Climatology* **19**: 513–536.

Enfield DB, Mestas-Nuñez AM, Trimble PJ. 2001. The Atlantic multidecadal oscillation and its relation to rainfall and river flows in the continental U.S. *Geophysical Research Letters* **28**: 2077–2080.

Enfield DB, Mestas-Nuñez AM, Mayer DA, Cid-Serrano L. 1999. How ubiquitous is the dipole relationship in tropical Atlantic sea surface temperature? *Journal of Geophysical Research* **104**: 7841–7848.

Goddard S, Mason SJ, Zebiak SE, Ropelewski CF, Basher R, Cane MA. 2001. Current approaches to seasonal-to-interannual climate predictions. *International Journal of Climatology* **21**: 1111–1152.

Hansen J, Ruedy R, Glascoe J, Sato M. 1999. GISS analysis of surface temperature change. *Journal of Geophysical Research* **104**: 30997–31022.

Kang IS, Baek HJ. 1993. Long-range prediction of winter monthly-mean temperature in Korea. *Journal of the Korean Meteorological Society* **29**: 253–262.

Kim MK. 2003. Seasonal prediction of regional temperature in Korea using the lag-correlated large-scale predictors. *Journal of the Korean Meteorological Society* **39**: 347–357.

Kim MK, Kang IS, Park CK, Kim KM. 2004. Superensemble prediction of regional precipitation over Korea. *International Journal of Climatology* **24**: 777–790.

Lloyd-Hughes B, Saunders MA. 2002. Seasonal prediction of European spring precipitation from El Niño-southern oscillation and local sea-surface temperatures. *International Journal of Climatology* **22**: 1–14.

Michaelsen J. 1987. Cross-validation in statistical climate forecast models. *Journal of Applied Meteorology* **26**: 1589–1600.

Mo KC. 2003. Ensemble canonical correlation prediction of surface temperature over the United States. *Journal of Climate* **16**: 1665–1683.

Moura AD, Hastenrath S. 2004. Climate prediction for Brazil's Nordeste : Performance of empirical and numerical modeling methods. *Journal of Climate* **17**: 2667–2672.

Palmer TN, Anderson DLT. 1994. The prospects for seasonal forecasting-A review paper. *Quarterly Journal of the Royal Meteorological Society* **120**: 755–793.

Qian B, Saunders MA. 2003. Summer U.K. temperature and its links to preceding Eurasian snow cover, North Atlantic SSTs, and the NAO. *Journal of Climate* **16**: 4108–4120.

Rasmusson EM, Carpenter TH. 1982. Variations in tropical sea surface temperature and surface wind fields associated with southern oscillation/El niño. *Monthly Weather Review* **110**: 354–384.

Schwing FB, Murphree T, Green PM. 2002. The Northern Oscillation Index (NOI): a new climate index for the northeast Pacific. *Progress in Oceanography* **53**: 115–139.

Singhrattna N, Rajagopalan B, Clark M, Kumar K. 2005. Seasonal forecasting of Thailand summer monsoon rainfall. *International Journal of Climatology* **25**: 649–664.

Thompson DWJ, Wallace JM. 2000. Annular modes in the extratropical circulation. Part I: month-to-month variability. *Journal of Climate* **13**: 1000–1016.

Wang C, Enfield DB. 2001. The tropical western hemisphere warm pool. *Geophysical Research Letters* **28**: 1635–1638.

Wilks DS. 1995. *Statistical Methods in the Atmospheric Sciences: An Introduction*. Academic press; 464.

Zhang Y, Wallace JM, Battisti DS. 1997. ENSO-like interdecadal variability: 1900-93. *Journal of climate* **10**: 1004–1020.